Gerade/ungerade symmetry-breaking in HD at the $n = 2$ dissociation limit

A. de Lange, E. Reinhold, W. Hogervorst, and W. Ubachs

Abstract: We report on a study of the $I'^{1}\Pi_g$ outer well state of HD. Via a resonance-enhanced XUV + IR (extreme ultraviolet + infrared) excitation scheme, rovibronic levels ($v = 0$–2, $J = 1$–4) are populated and probed by pulsed lasers. Level energies are measured with an accuracy of ≈0.03 cm^{-1}. Due to gerade–ungerade symmetry breaking, the long-range behavior of the I' potential in HD deviates from that of H_2 and D_2. When this deviation is taken into account a semi-empirical potential for the $I'^{1}\Pi_g$ state may be constructed, resulting in better agreement with the observed level energies than derived from an adiabatic ab initio potential. With this new potential it is predicted that the I' well can sustain only 4 vibrational levels, with the $v = 3$ level having a binding energy of ≈1.38(3) cm^{-1}.

PACS Nos.: 33.80.Rv, 34.20.Cf, 33.20.Ni, 31.50.+w

Résumé: Nous étudions ici l'état $I'^{1}\Pi_g$ de la molécule HD. Via une méthode d'excitation augmentée d'une résonance XUV-IR (ultraviolet lointain et infrarouge), nous peuplons les états de rotation-vibration ($v = 0$–2, $J = 1$–4) que nous sondons par laser pulsé. L'énergie laser est mesurée avec une précision ≈0.03 cm^{-1}. À cause du bris de symétrie gauche–droite, la partie longue portée du potentiel I' de HD diffère des cas H_2 et D_2. Tenant compte de cette déviation, il est possible de construire un potentiel semi-empirique pour l'état $I'^{1}\Pi_g$, résultant en un meilleur accord avec la valeur observée qu'en utilisant un potentiel postulé adiabatique dès le départ. Avec ce nouveau potentiel, nous prédisons que le puits I' ne peut avoir que quatre (4) états vibrationnels, l'état $v = 3$ ayant une énergie d'environ ≈1.38(3) cm^{-1}.

[Traduit par la rédaction]

1. Introduction

The present study deals with a laser spectroscopic investigation of quantum states in the HD molecule pertaining to the shallow outer well part of the $I\,I'^{1}\Pi_g$ potential. This study is connected to the work of Professor Stoicheff in more than one way. The Stoicheff group has taken part in the development of narrowband tunable extreme ultraviolet (XUV) laser radiation sources based on nonlinear optic conversion in gases. After initial work on wave-mixing in metal vapors [1–5] and molecular gases [6] resonance-enhanced sum-frequency mixing processes in noble gases were studied. Tunable narrowband XUV light was applied by Stoicheff et al. in excitation studies of molecular hydrogen, resulting in

Received October 8, 1999. Accepted March 14, 2000. Published on the NRC Research Press Web site on June 23, 2000.

A. de Lange,[1] **E. Reinhold, W. Hogervorst, and W. Ubachs.** Department of Physics and Astronomy, Vrije Universiteit, De Boelelaan 1081, 1081 HV Amsterdam, the Netherlands.

[1] Corresponding author: FAX: +31 20 444 7999; e-mail: arno@nat.vu.nl

the celebrated work on the accurate determination of the dissociation limit in H_2, D_2 and HD from measurements of the onset of dissociation at the $n = 2$ limit [7–10]. Here we report on XUV-IR double resonance excitation of HD just below the $n = 2$ dissociation limit, using a similar narrowband tunable XUV-source in conjunction with a pulsed infrared laser.

The lowest $^1\Pi_g$ potential in molecular hydrogen features a double-well structure in the representation of adiabatic potentials. Mulliken suggested in 1964 [11] the existence of a shallow outer well, reasoning that the long-range interaction of the atomic orbitals H(1s) and H(2p) in the $^1\Pi_g$-type superposition is attractive [12] and that the lowest possible $^1\Pi_g$ state in the molecular-orbital basis is $1s\sigma_g 3d\pi_g$, an $n = 3$ Rydberg state with a potential above the $n = 2$ dissociation limit at moderately large internuclear distances R. Due to the noncrossing rule, both must be connected at large R, forming a single adiabatic potential. The outer well is separated from the inner well by a barrier, which reaches a value of $\approx$1850 cm^{-1} above the dissociation limit [13]. Therefore, the vibrational states are almost completely localized in either one of the wells and separate sets of quantum numbers are used for the I (inner well) and I' (outer well) states, following the nomenclature of Yu and Dressler [14].

Recently we reported on the investigation of the I' state in the isotopomers H_2 and D_2 [15]. In the present study, we report on the observation of rovibrational levels in the I' state of the HD isotopomer. Energies of $v = 0$–2 and $J = 1$–4 levels of (e) and $J = 2, 3$ levels of (f) electronic symmetry are determined and show larger deviation from the ab initio calculations in the adiabatic representation [13] than level energies in H_2 and D_2.

In diatomic molecules, a symmetry operation i can be defined, inverting the electronic part of the wave function with respect to the geometrical center of the molecule. Because of the invariance of the Coulomb field under i in homopolar molecules, the electronic states are divided into two classes of eigenstates of i: "g" (gerade) and "u" (ungerade) with eigenvalues $+1$ and -1, respectively. In the Born–Oppenheimer approximation the g/u symmetry holds exact, even for hetero-isotopic molecules. The only term in the total Hamiltonian of homonuclear molecules that does not commute with the operator i, is the hyperfine interaction term, involving nuclear spin. In hydrogen this interaction is weak (< 0.1 cm^{-1}) near the $n = 2$ dissociation limit and the g/u label is, in high approximation, a good quantum number. In hetero-isotopic molecules however, an additional g/u symmetry-breaking term enters the Hamiltonian [16]:

$$H_{\mathrm{gu}} = \hbar^2 \frac{M_1 - M_2}{2M_1M_2} \nabla_{\boldsymbol{R}} \cdot \sum_j \nabla_j \tag{1}$$

Here $\boldsymbol{R}$ refer to the nuclei and the index j runs over all electronic coordinates. This term, representing the coupling of electronic motion with the asymmetric nuclear motion around the centre of mass, may be significant and causes breakdown of the adiabatic representation close to the second dissociation limit where the energy splitting between interacting configurations is 20 cm^{-1} (the splitting of H(2p) + D(1s)/H(1s) + D(2p)) over a wide range of internuclear distances. This is a considerable contribution in the I' outer well when compared to the potential depth of $\approx$ 200 cm^{-1}. Due to this symmetry breaking the accuracy of the predicted level energies within the adiabatic approximation is in poorer agreement with the observed level energies in HD than in the case of H_2 and D_2.

We have constructed a semi-empirical potential, demonstrating that, when accounting for mixing with the $C\,^1\Pi_u$ state, better agreement is achieved between calculated and measured values. Within the adiabatic representation the vibrational levels $v > 2$ lie above the lower of the two dissociation limits, but with the constructed potential it is calculated, though unobserved, that the vibrational level $v = 3$ should be bound. In addition to the I' resonances, a rotational progression is observed, which can be assigned as the $EF\,^1\Sigma_g^+$, $v = 37$ vibrational level.

Fig. 1. Overview XUV + IR spectrum of HD with the XUV laser tuned on the $B\,^1\Sigma_u^+$–$X\,^1\Sigma_g^+$ (18, 0) $R(0)$ transition. The traces show, respectively, the H^+ and D^+ ion signals obtained after the ionization pulse. The lines are saturation broadened. The continuum onset in the upper trace corresponds to the H^* + D dissociation limit, whereas the onset in the second trace corresponds to the H + D^* dissociation limit. The feature superimposed on the continuum signal in the upper trace, is due to an unassigned predissociating state. The line marked with an asterisk is unidentified.

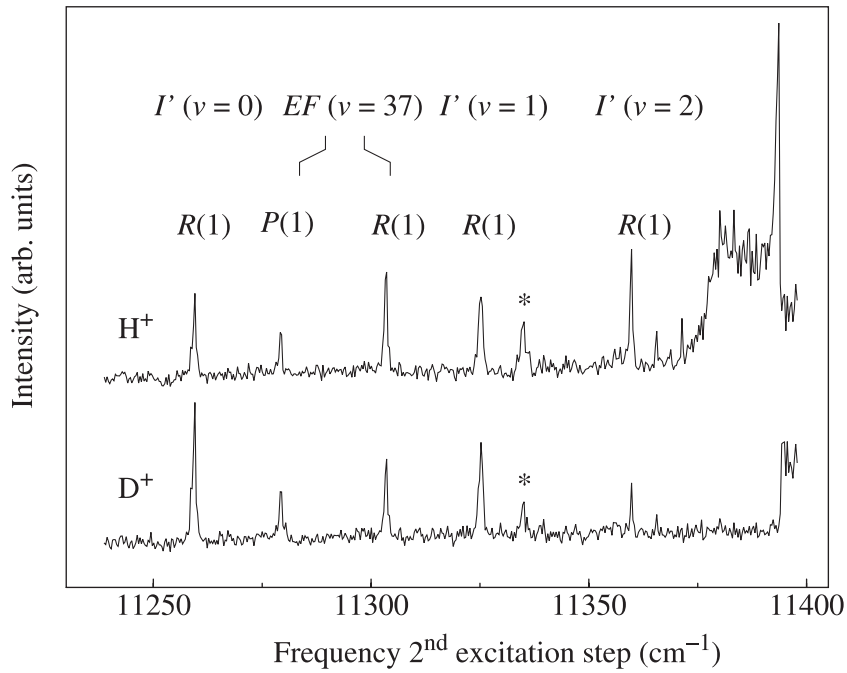

2. Experiment

The experimental setup is similar to the one used for the investigation of the I' state in the homonuclear isotopomers [15]. Two laser pulses in the XUV (extreme ultraviolet) and IR (infrared), driving a resonance-enhanced two-photon transition with $B\,^1\Sigma_u^+$ ($v = 18$) as intermediate, are used to populate rovibrational levels in the I' state. A third probe laser pulse (355 nm) excites the HD molecules, prepared in the I' state, into the dissociation continuum of HD^+ forming either H^+ or D^+. The ions are mass-selected by means of a time-of-flight tube and detected by an electron multiplier. The IR ($\lambda \approx 885$ nm) and the 355 nm beams are spatially overlapped with the counter-propagating XUV beam ($\lambda \approx 93$ nm), intersecting a molecular beam in the interaction region. As in the previous study on H_2 and D_2 [15], the XUV and the IR beams must be temporally overlapped as the lifetime of the B state is $\approx$1 ns. In H_2 and D_2 the I' state has a long lifetime (>100 ns), because fluorescence to the X ground state is prohibited by the g $\not\leftrightarrow$ g dipole selection rule; so the probe laser could be delayed without significant loss of signal. In the case of HD, however, the 355 nm beam can only be delayed a mere 4 ns for optimal S/N ratio, since the lifetime of the I' state is shorter in HD than in H_2 and D_2 due to the fact that the g/u symmetry is here not strictly valid. At a reduced delay of 4 ns, partial temporal overlap between the XUV and 355 nm beam causes some parasitic H^+ and D^+ background signal. Apart from the signal associated with molecular resonances, H^+ and D^+ are also produced because of the ionization of atomic fragments; this occurs when the energy of the second laser is sufficient to reach the ($n = 2$) dissociation limit. Both H($n = 2$) and D($n = 2$) dissociation products are then ionized by the 355 nm laser.

Fig. 2. Detailed XUV + IR spectrum (upper part) and Te_2 absorption spectrum of the frequency-doubled IR (lower part). The XUV laser is tuned on the $B\,^1\Sigma_u^+$–$X\,^1\Sigma_g^+$ (18, 0) $R(0)$ transition. The depicted line corresponds to the $I'\,^1\Pi_g$–$B\,^1\Sigma_u^+$ (1, 18) $R(1)$ transition. The intensity of the IR radiation is reduced such that the line is only slightly saturation-broadened. The background signal on which the line is superimposed arises from multi-photon ionization of the B state by the 355 nm pulse since there is partial temporal overlap between the XUV and the 355 nm beams. The Te_2 absorption lines used for calibration are marked with an asterisk.

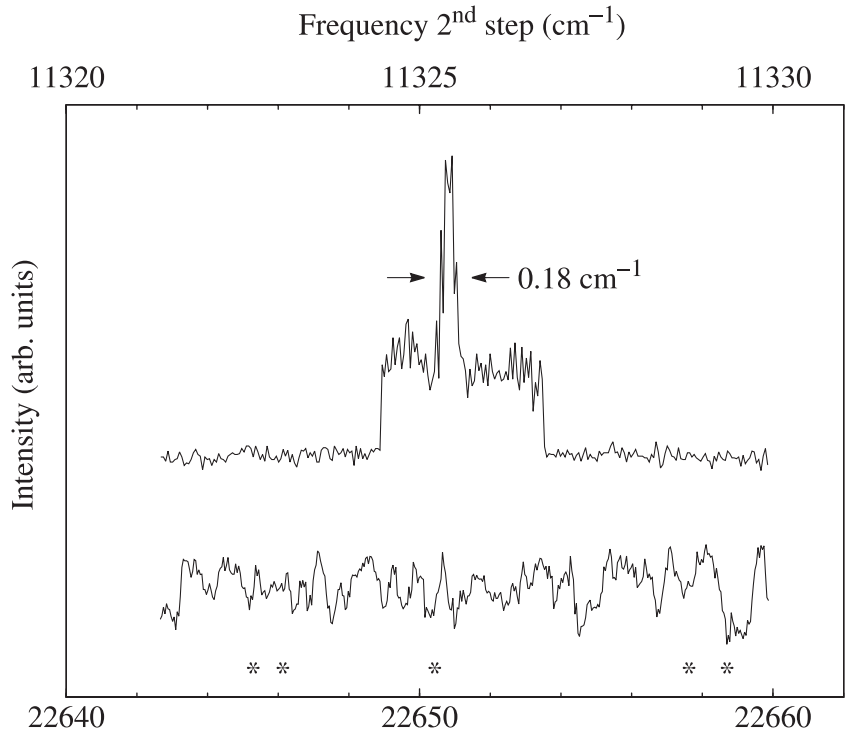

The spectra are recorded in two stages. Firstly, an overview scan is made at high IR intensities. A second scan is made with reduced IR intensity to avoid saturation-broadening effects. The traces in Fig. 1 show the H^+ and D^+ yield during an overview scan with the XUV radiation tuned on the B–X (18, 0) $R(0)$ transition. In case of the $I'\,^1\Pi_g$–$B\,^1\Sigma_u^+$ system P, Q, and R transitions are in principle allowed; however, the $P(1)$ transition would probe a $J = 0$ level, which does not exist in a Π state, whereas the $Q(1)$ transition is forbidden due to m selection rules in combination with the parallel polarizations of the XUV and IR beams. Therefore, only the $R(1)$ transitions are observed in this case, as can be seen in Fig. 1. In addition to molecular resonances, the dissociation onsets of the $n = 2$ limit are observable as well. To obtain total level energies, only the IR radiation has to be calibrated as the rovibrational energies of the B state are known up to 0.03 cm^{-1} [17]. In the infrared near 885 nm no standard reference is readily available and the IR radiation is frequency-doubled to record a Te_2 spectrum simultaneously with the double resonance spectra. By fitting the absorption lines to Gaussian profiles and assigning the peak positions with the Te_2-atlas [18], an accurate frequency scale is constructed in the IR. In Fig. 2 a scan with reduced IR intensity is depicted together with the calibration spectrum.

3. Results and discussion

All observed transition frequencies are listed in Table 1, with their assignments as discussed below. Total level energies with respect to the ground state, listed in Tables 2 and 3, are obtained by adding

Table 1. Transition frequencies ν (in cm^{-1}) of the second excitation step from $B\,^1\Sigma_u^+$ ($v = 18$, J) intermediate levels together with the assignment of the upper levels.

ν	Level	J'	ν	Level	J'	ν	Level	J'
via B ($J = 0$)			via B ($J = 2$)			via B ($J = 3$)		
11 271.53	$I'0$	1	11 222.37	$I'0$	1	11 178.01	$I'0$	2
305.85	$EF37$	1	227.20	$I'0$	2	185.20	$I'0$	3
373.91	$I'2$	1	234.27	$I'0$	3	194.40	$I'0$	4
			256.67	$EF37$	1	221.68	$EF37$	2
via B ($J = 1$)			285.85	$EF37$	3	243.55	$I'1$	2
			288.39	$I'1$	1	248.94	$I'1$	3
11 259.93	$I'0$	2	292.73	$I'1$	2	254.08	$EF37$	4
279.56	$EF37$	0	297.97	$I'1$	3	255.48	$I'1$	4
303.59	$EF37$	2	324.55[a]	$I'2$	1	277.97	$I'2$	2
325.41	$I'1$	2	327.04	$I'2$	2	280.33	$I'2$	3
359.90	$I'2$	2	329.37	$I'2$	3	284.36	$I'2$	4

[a] Very weak, not used in rotational fit.

Fig. 3. Rovibronic energies of the I', $v = 0$–2 state and the EF, $v = 37$ state, as a function of $J(J + 1)$. The indicated binding energies are with respect to the H($n = 2$) + D($n = 1$) dissociation limit. The deviation of the vibrational level EF ($v = 37$) from a straight line indicates strong nonrigidity of the rotational motion.

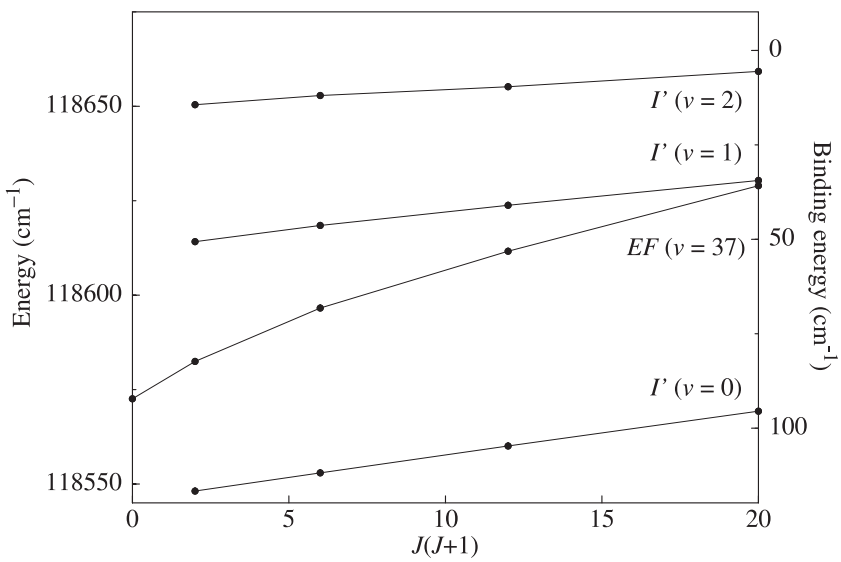

the measured transition frequencies in the IR to the energies of the intermediate B levels; the latter are obtained by adding B–X (18, 0) transition frequencies from ref. 17 to the ground-state rotational energies from ref. 19. Unambiguous assignment of rovibrational $I'\,^1\Pi_g$ levels is possible for $v = 0$–2, $J = 1$–4 (e electronic parity) and $J = 2, 3$ (f parity). In Fig. 3, the excitation energies, as well as the bonding energies of the observed levels are plotted as a function of $J(J + 1)$.

A rotational analysis is performed for all observed vibrational levels $v = 0$–2. The level energies of

Table 2. Energies of the $I'\,^1\Pi_g$ levels relative to the $X\,^1\Sigma_g^+$ ($v = 0$, $J = 0$) ground state. E_{calc} are the calculated energy eigenvalues in the constructed semi-empirical potential as explained in the text. All values in cm^{-1}.

		(e) levels			(f) levels		
J	E_{calc}	E_{obs}	Δ^a_{oc}	Δ^b_{oc}	E_{obs}	Δ^a_{oc}	Δ^b_{oc}
$v = 0$							
1	118 548.33	118 548.14	−0.19	−0.69			
2	553.11	552.92	−0.19	−0.69	118 552.95	−0.16	−0.66
3	560.20	560.05	−0.15	−0.68	560.03	−0.17	−0.70
4	569.55	569.30	−0.25	−0.79			
$v = 1$							
1	118 615.36	118 614.17	−1.19	−1.83			
2	618.81	618.43	−0.38	−1.02	118 618.47	−0.34	−0.98
3	623.89	623.75	−0.14	−0.79	623.75	−0.14	−0.79
4	630.50	630.38	−0.12	−0.77			
$v = 2$							
1	118 650.13	118 650.51	0.38	−0.46			
2	652.26	652.89	0.63	−0.85	118 652.91	0.65	−0.83
3	655.31	655.15	−0.16	−1.17	655.43	0.12	−0.89
4	659.14	659.26	0.12	−1.07			
$v = 3$							
1	118 663.42						
2	664.29						

Δ^a_{oc} = Observed–calculated (semi-empirical potential; this work)
Δ^b_{oc} = Observed–calculated (adiabatic ab initio potential [13])

Table 3. Level energies of the $EF\,^1\Sigma_g^+$ ($v = 37$) state relative to the $X\,^1\Sigma_g^+$ ($v = 0$, $J = 0$) ground state. All values in cm^{-1}.

J	E_{obs}
0	118 572.56
1	582.45
2	596.59
3	611.63
4	628.98

both (e) and (f) parity components, are fitted simultaneously to the formulae:

$$E^f_{vJ} = \nu_v + B_v[J(J+1) - \Lambda^2] - D_v[J(J+1) - \Lambda^2]^2 \quad (2)$$

$$E^e_{vJ} = E^f_{vJ} + Q_v J(J+1) \quad (3)$$

The resulting fitting parameters are tabulated in Table 4. A $\chi^2 \approx 1$ per point for $v = 0$ is obtained with an error in the transition frequencies of 0.03 cm^{-1}. A small value for the Λ-doubling ($Q_v < 0.05\ cm^{-1}$) indicates that systematic heterogeneous interaction of the (e) levels with the $^1\Sigma_g^+$ manifold is weak, as in H_2 and D_2 [15]. The analysis for $v = 1$ results in a χ^2 value of ≈13 per point, based on an error of

Table 4. Results of the rotational analysis of the vibrational levels of the I', $v = 0$–2 states according to (2) and (3). All values in cm^{-1}.

v	ν_v	B_v	$D_v/10^{-3}$	$Q_v/10^{-3}$
0	118 546.93	1.217	1.7	−7
1[a]	118 613.81	0.955	3.8	−10
2[b]	118 650.1	0.51	3	2

[a] $J = 1$ is not included in the fitting procedure as is explained in the text.
[b] $\chi^2 \approx 100$ per point, with an error of 0.03 cm^{-1}.

0.03 cm^{-1}. Furthermore, the value of D_v is one order of magnitude larger than in the case of H_2 and D_2. By excluding $J = 1$ from the fit, this deficit can be restored, but the fit itself becomes unreliable as the number of level energies is five and the number of parameters is four. The deviation from the fit for $J = 1$ is ≈0.6 cm^{-1}. Probably, this discrepancy is due to an accidental interaction with a state of either gerade or ungerade symmetry. If the analysis is applied to $v = 2$, the resulting χ^2 value is ≈100 per point (based on an error of 0.03 cm^{-1}), indicating a strong deviation from an unperturbed rotational progression. Indicative for this deviation is the accidental Λ-doubling of 0.3 cm^{-1} for $J = 3$. Also this perturbation may be due either to a gerade or an ungerade state.

A model is developed to describe I' levels, based on existing ab initio calculations, but taking the asymmetry of the HD isotopomer explicitly into account. The most recent ab initio calculations in the adiabatic representation for the $II'\,^1\Pi_g$ potential by Dressler and Wolniewicz [13] give binding energies with respect to the $(n = 1) + (n = 2)$ dissociation limit. As the g/u symmetry holds in the adiabatic approximation for all isotopomers, including HD, the configuration at the dissociation limit is a superposition with an energy halfway between H* + D and H + D*, which is called the adiabatic dissociation limit. The adiabatic representation will break down when the binding energies are of the same order of magnitude or less than the splitting of the two ways of dissociation. However, even the calculated rotational levels of the lowest vibrational level differ more from the experimental values in HD (typically 0.7 cm^{-1}, as can be seen in Table 2) than in the other two isotopomers (typically 0.1 cm^{-1} [15]).

Due to the g/u symmetry-breaking term given by (1), the long-range behavior of the I' state in HD differs significantly from that in H_2 and D_2. The $I'\,^1\Pi_g$ state correlates with 1s + 2p dissociation fragments, with the 2p-atom in a π-orientation with respect to the internuclear axis; the asymptotic electronic wave function of the I' state (as well as that of other states correlating with the same limit) can thus be written as a sum over products of one-electron wave functions of these atomic states. In the approximation of negligible spin-orbit interaction spatial and spin parts are separable, so the foregoing holds for the spatial wave function Φ alone. The one-electron basis functions of Φ are denoted as $\phi_{1s,n}(i)$ and $\phi_{2p\pi,n}(i)$, where i numbers the electrons and n the nucleus at which it is located (for the relative signs of the $\phi_{2p\pi,n}$ orbitals we assume parallel orientation in space for the coordinate systems at the nuclei); the two-electron wave function is then given by

$$\Phi = c_{11}\phi_{1s,1}(1)\phi_{2p\pi,2}(2) + c_{12}\phi_{1s,1}(2)\phi_{2p\pi,2}(1) + c_{21}\phi_{1s,2}(1)\phi_{2p\pi,1}(2) + c_{22}\phi_{1s,2}(2)\phi_{2p\pi,1}(1) \quad (4)$$

Antisymmetrization of the total wave function under electron exchange requires $c_{11} = c_{12}$, $c_{21} = c_{22}$ for singlet states and $c_{11} = -c_{12}$, $c_{21} = -c_{22}$ for triplet states; inversion symmetry with respect to the geometrical center of the molecule requires $c_{11} = c_{21}$, $c_{12} = c_{22}$ for ungerade states and $c_{11} = -c_{21}$, $c_{12} = -c_{22}$ for gerade states. For the $I'\,^1\Pi_g$ state this leads to $c_{11} = c_{12} = -c_{21} = -c_{22}$; similar

relations hold for the three other states of well-defined symmetries that can be built from (4). In HD at the H*($n = 2$) + D($n = 1$) dissociation threshold the inversion symmetry requirement is relaxed. Instead, a different condition has to be fulfilled: the wave function cannot contain contributions with excitation of the electron at the deuteron (which we may label nucleus 1), i.e., $c_{21} = c_{22} = 0$; this conclusion is not affected by the possibility of enlarging the basis state set beyond 4 by including other atomic configurations. From the relations given above it can be seen that any state at the H* + D limit which (expressed in the basis with well-defined symmetries) has an I' contribution must have an equal contribution of the singlet ungerade state, which is the $C\,^1\Pi_u$ state. At finite internuclear distances, where adiabatic I' and C potentials shift apart, the excitation becomes less localized at the H atom. This effect is observed in the present experiment; the H^+/D^+ signal ratio shifts from 2/3 ($v = 0$) via 1 ($v = 1$) to 2 ($v = 2$), as can be seen in Fig. 1 and in other recorded spectra.

Neglecting interactions with other states, the following eigenvalue problem has to be solved to investigate the long-range behavior of the I' potential in HD

$$\begin{pmatrix} V_C(R) & \Delta E \\ \Delta E & V_{I'}(R) \end{pmatrix} \Psi(R) = E(R)\Psi(R) \tag{5}$$

with the asymptotic adiabatic potentials

$$V_C = \frac{C_3}{R^3} - \frac{C_6}{R^6} - \frac{C_8^{\mathrm{u}}}{R^8} \tag{6}$$

$$V_{I'} = -\frac{C_3}{R^3} - \frac{C_6}{R^6} - \frac{C_8^{\mathrm{g}}}{R^8} \tag{7}$$

with respect to the adiabatic dissociation limit. The coefficients $C_3 = 1.218\,923\,22 \times 10^5$ cm$^{-1}\,a_0^3$, $C_6 = 2.077\,337 \times 10^7$ cm$^{-1}\,a_0^6$, $C_8^{\mathrm{u}} = 3.573\,309 \times 10^8$ cm$^{-1}\,a_0^8$ and $C_8^{\mathrm{g}} = 2.327\,982 \times 10^8$ cm$^{-1}\,a_0^8$ correspond to the Π-type long-range 1s + 2p interaction of a H-atom with a D-atom calculated from the values of the interaction between two H-atoms [20], taking into account the nuclear-mass dependence of the Rydberg constant. It is noted that in ref. 20 the internuclear distance is given in atomic units for the real hydrogenic system and not in terms of Bohr-radii (a_0), i.e., the unit scales with the reduced mass. We convert the scale into units of a_0 to make it consistent with the scale of the ab initio potential [13].

The value of ΔE equals the difference between the adiabatic dissociation limit and one of the actual limits, i.e., half the difference between the energies of H (1s) + D (2p) and H (2p) + D (1s). This value ($\Delta E = 11.19$ cm^{-1}) is determined using the value of the hydrogen–deuterium isotope shift of the 1S–2S transition as given in ref. 21 with neglect of the fine-structure; this splitting is the same for both isotopes up to an accuracy of 0.001 cm^{-1} [22]. Because of the fact that the potential energies corresponding to the C state are higher than the I' state at moderately large values of R, and because of the noncrossing rule, the lower of the two potentials found after diagonalization of matrix (5), correlates to the I' potential for HD:

$$V = -\frac{C_6}{R^6} - \frac{C_8^{\mathrm{g}} + C_8^{\mathrm{u}}}{2R^8} - \sqrt{\left(\frac{C_3}{R^3} + \frac{C_8^{\mathrm{g}} - C_8^{\mathrm{u}}}{2R^8}\right)^2 + (\Delta E)^2} \tag{8}$$

For large R this potential reduces to

$$V \approx -\Delta E - \left(C_6 + \frac{C_3^2}{2\Delta E}\right) R^{-6} + \mathcal{O}\left(R^{-8}\right) \tag{9}$$

It is noted that the R^{-6} potential does not purely originate from a van der Waals interaction but also contains a part associated with g/u mixing.

Fig. 4. The constructed semi-empirical I' potential (continuous line) coincides with the adiabatic potential (broken line) for small internuclear distance R. For larger values of R, due to break down of the g/u symmetry, the potential converges towards the lower of the two dissociation channels (H ($n = 2$) + D) with an R^{-6} dependence; the leading term is shown by a dotted line. The adiabatic dissociation limit has $E = 0$. The vibrational levels $v = 1, 2$ $J = 1$ of the I' state are also indicated. The $v = 2$ state is in the transition region from an R^{-3} to an R^{-6} dependence of the I' potential.

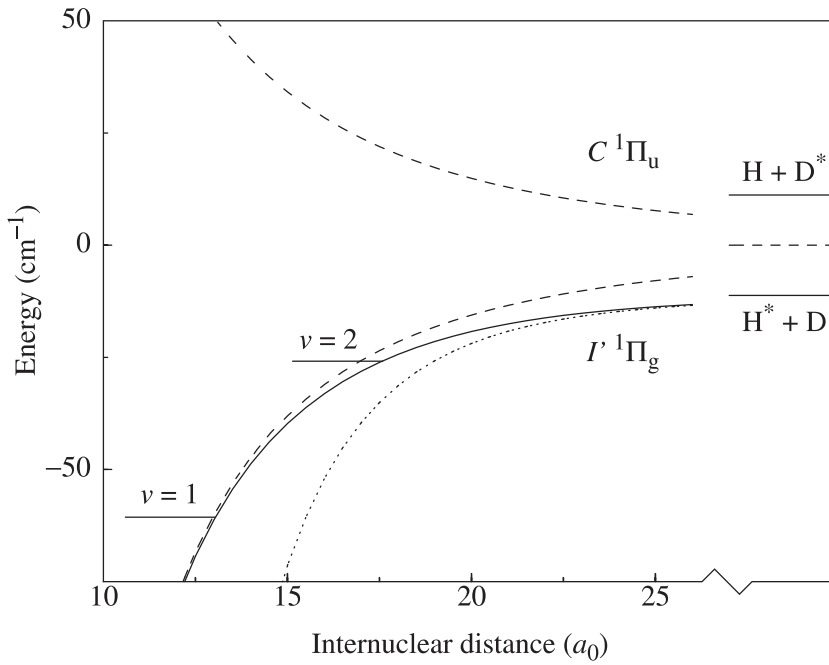

The I' potential in homonuclear isotopomers has a leading term of R^{-3} dependence representing a resonant dipole–dipole interaction, in contrast to HD. This marked distinction between HD on the one hand and H_2 and D_2 molecules on the other can be physically understood as follows. The atoms, respectively, in the 1s and 2p states, have no permanent dipole moment when isolated, but in the case of interacting identical atoms no distinction can be made as to which atom is excited and which one is in the ground state, giving rise to a superposition as is expressed in (4). The resulting atomic dipole moments, having a fixed relative orientation, give rise to the resonant dipole–dipole interaction [23]. In the case of HD however, no such superposition can exist and no resonant dipole moments can be formed, i.e., the R^{-3}-term must vanish. In Fig. 4, the resulting potential from (8) is depicted together with the adiabatic I' potential and the long-range approximation of (9). It is noted that, though in the picture of interacting atoms no dipole–dipole interaction between atomic constituents can occur in HD, the molecule itself may have a permanent electric dipole moment.

LeRoy and Bernstein [24] and Stwalley [25] have shown that the binding energies ε_v of vibrational levels v close to the dissociation limit of a potential that asymptotically follows a simple power law, $V = -C_n R^{-n}$, are related by

$$v_D - v \approx a_n \varepsilon_v^{(n-2)/2n} \tag{10}$$

with a_n a constant proportional to C_n and v_D the "effective" vibrational quantum number at the dissociation limit (not necessarily an integer). This formula yields that the potential well should sustain 6

vibrational levels in the case of H_2 and 10 in the case of D_2 [15]. For HD in the adiabatic approximation 8 levels are predicted. However, it is to be expected that the actual number of levels in HD will be less, because the vibrational states $v \geq 3$ of HD lie at a higher energy than the H* + D dissociation limit, which is lowered by 11.19 cm^{-1}. Moreover, the long-range behavior of the potential is not R^{-3}, as is the case with the other two isotopomers, but R^{-6}. The LeRoy–Bernstein analysis can also be applied to an R^{-6} potential, changing the exponent in (10) from 1/6 to 1/3. Approximating the I' potential with its pure R^{-6} asymptotic form beyond $v = 2$, it is estimated that one more vibrational level ($v = 3$) is bound. In the case of the I' state in HD, the behavior gradually changes from an R^{-3} to an R^{-6}-type potential and, with the highest of the observed vibrational levels still lying in the transition region, the analysis does not provide accurate level energies. To make this estimate more quantitative and to obtain a better agreement between calculation and measurements, a new potential is constructed using the ab initio adiabatic potential as given in ref. 13 for the inner part (4.75–12 a.u.) and the long-range potential of (8) for the outer part (>12 a.u.) to be used in a numerical calculation.

Firstly, adiabatic corrections are added to the Born–Oppenheimer energies, both calculated ab initio by Dressler and Wolniewicz [13], with the appropriate reduced mass of the nuclear motion in HD ($\mu_{HD} = 1223.8988$ a.u.) taken into account. Secondly, the long-range potential V of (8) is connected to the ab initio potential. At the connection point ($R = 12$ a.u.) the potential describing the outer part is $\approx$2.4 cm^{-1} lower in energy than the ab initio potential. In H_2 and D_2, however, this difference is merely $\approx$1.5 cm^{-1}, indicating that the adiabatic potential of I' in HD has to be corrected for the g/u-mixing already at intermediate internuclear distances. This is done by adding to the adiabatic potential of ref. 13 the difference between the power series of the adiabatic potential $V_{I'}$ of (7) and the corrected potential V of (8) (obtained after diagonalizing the matrix in (5)) extended to $R < 12$ a.u. This difference gives the correct shift at 12 a.u. and quickly converges to zero for small internuclear distances, correcting only the outer part of the well significantly ($\approx$1 cm^{-1}). Then a discontinuity of 1.5 cm^{-1} remains, which is isotope independent.

To overcome this difference in energy, the potential of (8) is adjusted, such that the two potentials are connected without a discontinuity at $R = 12$ a.u. and that the dissociation energy and the relevant terms in the long-range potential are unaffected. We have chosen, arbitrarily, to add an R^{-12} function with $C_{12} = 2.82 \times 10^{16}$ cm^{-1} a_0^{12} to the outer part of the potential, which satisfies these requirements.

Using this potential, vibrational levels are obtained with the program LEVEL 6.1 of LeRoy [26]. As can be seen in Table 2, the calculated level energies are in better agreement with the measured energies than the adiabatic level energies predicted by Dressler and Wolniewicz [13].

In addition to the observed vibrational levels, a fourth level ($v = 3$), with only two rotational levels $J = 1, 2$, is numerically calculated with a binding energy of 1.38 cm^{-1} ($J = 1$) with respect to the H* + D dissociation limit. The measured binding energies differ $\approx$1–2% with respect to the calculated ones, which implies an estimated absolute uncertainty of 0.03 cm^{-1} for the calculated upper level. As an additional check that $v = 3$ is the highest bound state, the LeRoy–Bernstein analysis starting from this level is applied to the asymptotic R^{-6} potential, as given in (9), which is a good approximation in this energy region. This results in an effective vibrational quantum number $v_D = 3.72$ at the dissociation limit, indicating that $v = 3$ is indeed the upper vibrational level.

In the current experiment the $v = 3$ vibrational level is not observed. It is to be expected that the transition to this vibrational level from the B ($v = 18$) state is weaker than to $v = 0$–2; the I' state is predominantly populated via the inner turning points of the vibrational levels ($R \approx 7.0$ a.u.), whereas the wave function density will be located more at the outer turning point for higher vibrational levels. This reduces the Franck–Condon overlap with the B ($v = 18$) state (one order of magnitude decrease is calculated between $v = 0$ and $v = 3$). Furthermore, detection by delayed photo-ionization may be hampered by lifetime shortening of $v = 3$ with respect to the other levels, since the g/u symmetry is more severely broken at large R and hence electric dipole radiation to the electronic ground state becomes possible as a competitive process.

In the above calculations binding energies are given with respect to the adiabatic dissociation limit, which is not an observable quantity. To determine the total level energies, as given in Table 2, a value for the adiabatic dissociation limit has to be invoked, which can be obtained, for example, by adding $\Delta E = 11.19$ cm^{-1} to the H$^*(n = 2)$ + D energy, the lower of the two real dissociation limits. The most accurate determinations of this limit are 118 664.78(7) cm^{-1} by Balakrishnan et al. [9] and 118 664.84(10) cm^{-1} by Eyler and Melikechi [27]. The weighted average of those values is used, i.e., 118 664.80 cm^{-1}. Hence, the adiabatic dissociation limit used to determine the total level energies is 118 675.99 cm^{-1}. An alternative way to determine the adiabatic dissociation limit would be to take the mean value of the two observed dissociation limits. However, it is noted that the splitting between both limits observed by Eyler and Melikechi [27] is consistent with the 1S–2S isotope shift, but the value found by Balakrishnan et al. [9] differs by ≈1 cm^{-1}. A possible explanation of this discrepancy in ref. 9 may be found in the fact that no discrimination can be made between H($n = 2$) and D($n = 2$) and a resonance in HD just below the upper dissociation limit may mask the true onset of this dissociation continuum. In Fig. 1 a resonance can be seen in the upper trace (H^+ signal) just below the D^+ onset in the lower trace.

In addition to the three vibrational levels in the I' potential, strong transitions belonging to a fourth rotational progression are observed. Total energies are given in Table 3. The binding energy of the lower rotational levels is ≈100 cm^{-1}, hence it is expected that g/u symmetry holds almost perfectly, except for accidental coincidences with the ungerade manifold, and thus the probed state belongs to the gerade class of singlet states. Four other singlet gerade states support bound states below the 1s $+2\ell$ limit; the $GK\,{}^1\Sigma_g^+$ state, the $EF\,{}^1\Sigma_g^+$ state, the $H\bar{H}\,{}^1\Sigma_g^+$ state and the $I\,{}^1\Pi_g$ state (the inner well of the II'). A Π state cannot support a $J = 0$ level, the lowest observed J value, and therefore the I state can be ruled out. Dressler and Wolniewicz have calculated rovibrational level energies for the EF, GK, and $H\bar{H}$ states for H_2, D_2 and HD in the adiabatic approximation [28]. Comparison between calculated and observed states just below the dissociation limit in H_2 and D_2 [15,29] shows a systematic overestimate ranging from 10–60 cm^{-1}. The observed level energy of 118 581.80 cm^{-1} ($J = 0$) is ≈52 cm^{-1} above the highest calculated vibrational level ($v = 9$) in the GK potential and the GK state is therefore left out of consideration. It is, however, ≈34 cm^{-1} below the calculated EF ($v = 37$) vibrational state and ≈52 cm^{-1} below the calculated $H\bar{H}$ ($v = 3$) state. The $H\bar{H}$ state can be ruled out on the basis of the value of the rotational constant. The value of the rotational constant $B \approx 3.9$ cm^{-1} of the observed rotational progression obtained from a fit to (2), corresponds to $\langle R^{-2} \rangle = 0.044$ a.u. This is more in agreement with the calculated values of the EF potential than with the $H\bar{H}$ levels [28]: 0.021 a.u. (EF ($v = 37$)) and 0.205 a.u. ($H\bar{H}$ ($v = 3$)), suggesting that the observed progression may correspond to the EF ($v = 37$) state. The rotational B-constant is of indicative value only, because fitting to (2) results in a $\chi^2 \approx 950$ per point (error of 0.03 cm^{-1}); see also Fig. 3. The deviations of the observed energies from the fit show unsystematic behavior, probably due to nonadiabatic interactions with other states. Therefore, including higher order centrifugal distortion terms does not substantially improve the fit.

4. Conclusion

Three vibrational states of the $I'\,{}^1\Pi_g$ state of HD within total 18 rovibrational levels, are observed in a resonance-enhanced XUV + IR excitation scheme. A semi-empirical potential is constructed, for which the breakdown of the gerade/ungerade symmetry in the long-range tail of the potential is taken into account. The inner part of the potential is taken from an ab initio calculation. With this potential it is predicted that a fourth vibrational level ($v = 3$), with only two rotational sublevels ($J = 1, 2$), should be confined in the potential well. The binding energy for $J = 1$ is calculated at 1.38(3) cm^{-1}. One more rotational progression is observed, which is tentatively identified as the $EF\,{}^1\Sigma_g^+$ ($v = 37$) state.

Acknowledgment

The authors wish to acknowledge the Netherlands Foundation for Fundamental Research on Matter (FOM) for financial support. They wish to thank R.J. LeRoy (Waterloo) for making available the LEVEL 6.1 software package.

References

1. T.J. McKee, B.P. Stoicheff, and S.C. Wallace. Opt. Lett. **3**, 207 (1978).
2. W. Jamroz, P.E. LaRocque, and B.P. Stoicheff. Opt. Lett. **6**, 461 (1981).
3. W. Jamroz, P.E. LaRocque, and B.P. Stoicheff. Opt. Lett. **7**, 617 (1982).
4. P.R. Herman, and B.P. Stoicheff. Opt. Lett. **10**, 502 (1985).
5. P.R. Herman, P.E. LaRocque, R.H. Lipson, W. Jamroz, and B.P. Stoicheff. Can. J. Phys. **63**, 1581 (1985).
6. K.K. Innes, B.P. Stoicheff, and S.C. Wallace. Appl. Phys. Lett. **29**, 715 (1976).
7. A. Balakrishnan, V. Smith, and B.P. Stoicheff. Phys. Rev. Lett. **68**, 2149 (1992).
8. A. Balakrishnan, and B.P. Stoicheff. J. Mol. Spectrosc. **156**, 517 (1992).
9. A. Balakrishnan, M. Vallet, and B.P. Stoicheff. J. Mol. Spectrosc. **162**, 168 (1993).
10. A. Balakrishnan, V. Smith, and B.P. Stoicheff. Phys. Rev. A: At Mol. Opt. Phys. **49**, 2460 (1994).
11. R.S. Mulliken. Phys. Rev. **138**, A962 (1964).
12. J.C. Browne. J. Chem. Phys. **41**, 1583 (1964).
13. K. Dressler and L. Wolniewicz. Can. J. Phys. **62**, 1706 (1984).
14. S. Yu and K. Dressler. J. Chem. Phys. **101**, 7692 (1994).
15. E. Reinhold, A. de Lange, W. Hogervorst, and W. Ubachs. J. Chem. Phys. **109**, 9772 (1998).
16. P.R. Bunker. J. Mol. Spectrosc. **46**, 119 (1973).
17. P.C. Hinnen, S.E. Werners, W. Hogervorst, S. Stolte, and W. Ubachs. Phys. Rev. A: At Mol. Opt. Phys. **52**, 4425 (1995).
18. J. Cariou and P. Luc. Atlas du spectre d'absorption de la molécule de tellure. Orsay, France. 1980.
19. P. Essenwanger and H.P. Gush. Can. J. Phys. **62**, 1680 (1984).
20. T.L. Stephens and A. Dalgarno. Mol. Phys. **28**, 1049 (1974).
21. A. Huber, Th. Udem, B. Gross, J. Reichert, M. Kourogi, K. Packucki, M. Weitz, and T.W. Hänsch. Phys. Rev. Lett. **80**, 468 (1998).
22. C.E. Moore. Atomic energy levels. National Bureau of Standards, Washington, U.S.A. 1971.
23. G.W. King and J.H. van Vleck. Phys. Rev. **55**, 1165 (1939).
24. R.J. LeRoy and R.B. Bernstein. J. Chem. Phys. **52**, 3869 (1970).
25. W.C. Stwalley. Chem. Phys. Lett. **6**, 241 (1970).
26. R.J. LeRoy. University of Waterloo Chem. Phys. Res. Rep. No. CP-555 (1995).
27. E.E. Eyler and N. Melikechi. Phys. Rev. A: At Mol. Opt. Phys. **48**, R18 (1993).
28. L. Wolniewicz and K. Dressler. J. Chem. Phys. **82**, 3292 (1984).
29. J. Ishii, K. Tsukiyama, and K. Uehara. Laser Chem. **14**, 31 (1994).